Saw-tooth softening model for reinforced concrete structures

J. G. Rots[1], B. Belletti[1,2], S. Invernizzi[1,3]

[1] Faculty of Architecture, Delft University of Technology (The Netherlands)
[2] Department of Civil and Environmental Engineering and Architecture, University of Parma (Italy)
[3] Department of Structural Engineering and Geotechnics, Politecnico di Torino (Italy)

ABSTRACT. *The non-linear behaviour of reinforced concrete structures strongly depends on abrupt cracking phenomena. The crack pattern prediction is fundamental to the reliable assessment of the structure, both at the service and at the ultimate limit states. The Non-linear Finite Element (NLFE) analysis is the common tool to perform these verifications. Unfortunately, the constitutive models for RC material are characterized by softening stress-strain relationships, which involve negative tangent stiffness. Therefore, the incremental-iterative solution procedure often leads to numerical instability and divergence problems, especially when the energy dissipated by cracking and crushing phenomena is little compared with the elastic energy stored in the structure. In this paper, the sequentially linear approach is proposed as an alternative to incremental convergence methods. The robustness and effectiveness of the method is proved through plane concrete and RC case studies.*

INTRODUCTION

In simulating the non-linear behaviour of the material RC, one has to use softening models, which involve negative tangent stiffness. Owing to these softening models the numerical solution, usually achieved by incremental-iterative procedures (e.g. Newton-Raphson), can encounter instability and divergence problems. These problems are independent on the type of smeared crack formulation adopted. For this reason, a solution procedure for finite element analysis is proposed as an alternative to incremental convergence methods [1], [2]. The incremental-iterative method is replaced by a series of linear analyses using a special scaling technique with subsequent stiffness/strength reduction per critical element. The structure is discretized using standard elastic continuum elements. Young's modulus, Poisson's ratio and initial strength are assigned to the elements. Subsequently, the following steps are sequentially carried out:

- Add the external load as a unit load.
- Perform a linear elastic analysis.
- Extract the 'critical element' from the results. The 'critical element' is the element for which the stress level divided by its current strength is the highest in the whole structure.
- Calculate the ratio between the strength and the stress level in the critical

element: this ratio provides the 'global load factor'. The present solution step is obtained rescaling the 'unit load elastic solution' times the 'global load factor'.

- Increase the damage in the critical element by reducing its stiffness and strength, i.e. Young's modulus E and strength, according to a saw-tooth constitutive law as described in the next section.
- Repeat the previous steps for the new configuration, i.e. re-run a linear analysis for the structure in which the material properties of the previous critical element have been reduced. Trace the next critical saw-tooth in the critical element, repeat this process till the damage has spread into the structure to the desired level.

The way in which the stiffness and strength of the critical elements are progressively reduced constitutes the essence of the model [3]. In other words, it is necessary to provide a saw-tooth approximation of the constitutive stress-strain relation.

CONSTITUTIVE MODEL ADOPTED FOR RC

An orthotropic fixed crack model based on total strain has been adopted in order to describe the constitutive behaviour of concrete. The following constitutive relation is assumed, being *n* the direction normal to the crack plane, and *t* the direction of the compressive struts:

$$\begin{Bmatrix} \sigma_{nn} \\ \sigma_{tt} \\ \sigma_{nt} \end{Bmatrix} = \begin{bmatrix} \dfrac{E_i \cdot E_j}{E_j - \nu^2 \cdot E_i} & \dfrac{\nu \cdot E_i \cdot E_j}{E_j - \nu^2 \cdot E_i} & 0 \\ \dfrac{\nu \cdot E_i \cdot E_j}{E_j - \nu^2 \cdot E_i} & \dfrac{E_j^2}{E_j - \nu^2 \cdot E_i} & 0 \\ 0 & 0 & \beta \cdot G \end{bmatrix} \begin{Bmatrix} \varepsilon_{nn} \\ \varepsilon_{tt} \\ \varepsilon_{nt} \end{Bmatrix}, \tag{1}$$

where E_i is the reduced Young's modulus in tension along the n-axis and E_j is the Young's modulus in compression along the t-axis.

Saw-Tooth Laws for Concrete in Tension

A saw tooth diagram has been defined for the non-linear tension softening curve shown in Fig. 1a. The curve, inspired to the bilinear Model Code (MC90) expression [4], has been formulated in its first version by Belletti, Cerioni and Iori [5] and partly modified to be easily implemented in the sequentially linear procedure.

The analytical expression is the following:

$$\sigma = f_t \left(\frac{1}{w} - \frac{1}{w_{eq}} \right) w, \tag{2}$$

where:

$$w_{eq} = \left(1 - \frac{w_1}{\delta \cdot w_c}\right) \cdot w + \frac{w_1}{\delta}, \tag{3}$$

where w_1 *and* w_c are the crack openings when σ is equal to $0.15\ f_t$ and to zero respectively. This non-linear tension softening has been modified in order to be implemented into the saw-tooth diagram. The first step is to formulate the presented non linear tension softening as a function of total strain rather than crack strain. The total strain is the sum of the elastic strain ε^e and the crack strain ε^{cr}:

$$\varepsilon = \varepsilon^e + \varepsilon^{cr} \quad \Rightarrow \quad \varepsilon^{cr} = \varepsilon - \frac{\sigma}{E}, \tag{4}$$

So, Eq. (3) can be expressed as a function of crack strain ε^{cr}, as follows, see [3]:

$$\sigma = f_t \left(1 - \frac{\varepsilon - \dfrac{\sigma}{E}}{\left(1 - \dfrac{w_1}{\delta \cdot w_c}\right) \cdot \left(\varepsilon - \dfrac{\sigma}{E}\right) + \dfrac{w_1}{\delta \cdot h}} \right), \tag{5}$$

After some algebraic manipulations, the strain-stress relation for concrete in tension is the following:

$$\sigma = \begin{cases} E \cdot \varepsilon & \Rightarrow for\ 0 \le \varepsilon \le \varepsilon_{cr} \\ \dfrac{B - \sqrt{B^2 - 4 \cdot A \cdot C}}{2 \cdot A} & \Rightarrow for\ \varepsilon_{cr} < \varepsilon \le \dfrac{w_c}{h} \\ 0 & \Rightarrow for\ \varepsilon > \dfrac{w_c}{h} \end{cases}, \tag{6}$$

the values of *A*, *B*, and *C* are reported into the nomenclature listed at the end of the paper.

As shown in Fig. 1a, a strength range is set, as a percentage of the maximum tensile strength. In other words, we introduce a band or ‘strip’ into the softening diagram, delimited by two curves parallel to and equidistant from the original branch. The number of required teeth (*N*) and the values of Young’s modulus (E_i) and tensile strength (f_{ti}) at the current stage *i* in the saw-tooth diagram are automatically obtained as values depending on this strength range, chosen by the user. The material properties reduction due to cracking of the “critical element” (i.e. the size and shape of each tooth) is determined by the lower softening tail (see Figure 1a):

$$f_{ti}^{-} = f_{ti}^{+} - 2pf_t, \tag{7}$$

The intersection between the nonlinear tension softening and the elastic loading branch gives the strain ε_i, from which follows the reduced Young's modulus:

$$\varepsilon_i = \frac{f_{ti}^{+}}{E_i} = \frac{f_{ti}^{-}}{E_{i+1}} \Rightarrow E_{i+1} = \frac{f_{ti}^{+} - 2pf_t}{f_{ti}^{+}} E_i \tag{8}$$

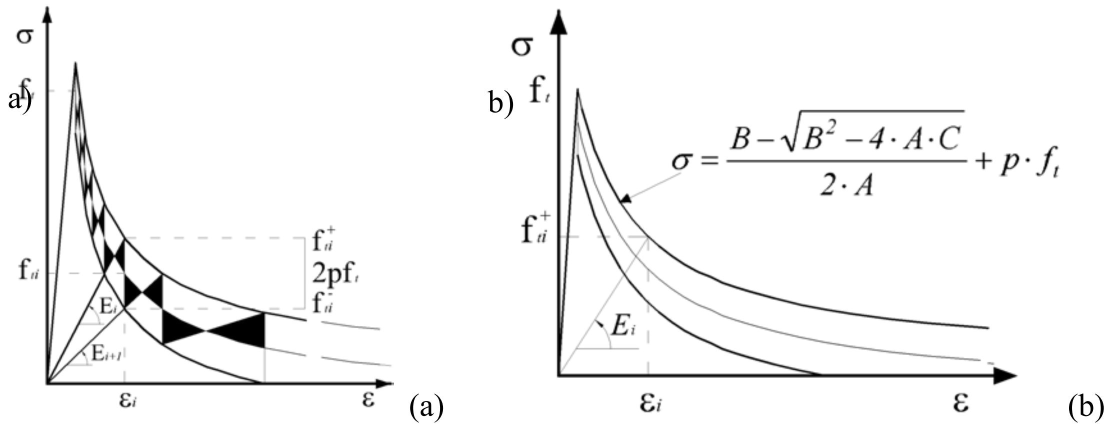

Figure 1. (a) Saw-tooth diagram for non-linear tension softening (a) and saw-tooth procedure. (b).

Adopting Eq.(6) and a value *p* of strength percentage, the corresponding uplifted stress is:

$$\sigma = \frac{B - \sqrt{B^2 - 4 \cdot A \cdot C}}{2 \cdot A} + p \cdot f_t \,. \tag{9}$$

The intersection point (see Fig. 1b) between the nonlinear tension softening and the elastic branch corresponding to the linear behavior of the current stage in the saw-tooth diagram, is the following:

$$\varepsilon_i = \frac{-b + \sqrt{b^2 + 4 \cdot a \cdot c}}{2 \cdot a} \Rightarrow f_{ti}^{+} = E_i \cdot \frac{-b + \sqrt{b^2 + 4 \cdot a \cdot c}}{2 \cdot a} \tag{10}$$

the values of *a*, *b*, and *c* are reported at the end, in the nomenclature list. The value of f_{ti}^{+} given by Eq. (10) can finally be substituted into Eq. (8) to obtain E_{i+1}.

Saw-Tooth Laws for Steel in Tension and compression

We adopt an elastic perfectly plastic stress-strain diagram for reinforcing steel both intension and compression, according to EC2 prescriptions [6], (see Fig. 2). The uplifted post peak curve is the following:

$$\sigma^{+} = (1 + p) f_y \tag{11}$$

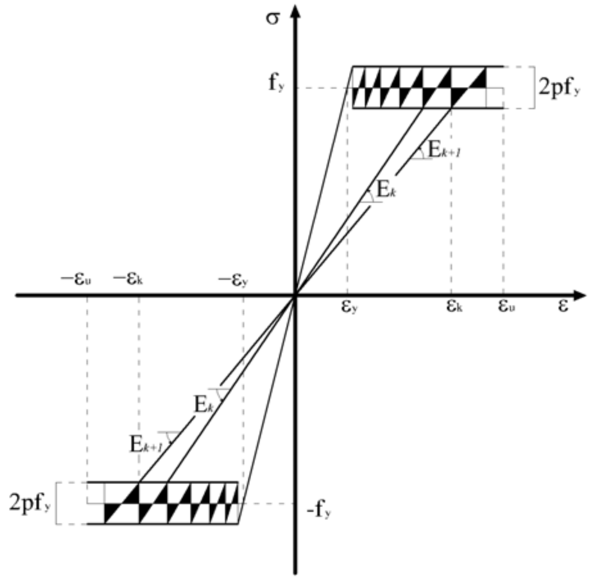

Figure 2. Mother curve and saw-tooth approximations for steel in compression and tension.

The intersection between the generic *k* secant elastic branch and the post peak plastic plateau is given by the following equation:

$$E_k \varepsilon_k = (1+p) f_y \Rightarrow \varepsilon_k = \frac{(1+p) f_y}{E_k} \qquad (12)$$

Finally, the updated (i.e. degraded) Young's modulus becomes:

$$E_{k+1} = \frac{(1-p) \cdot f_y}{\varepsilon_k} = E_k \frac{1-p}{1+p}; \quad 0 \le k \le L \qquad (13)$$

where *k*=*L* corresponds to complete damage of steel in tension or in compression.

CASE STUDIES: PLANE CONCRETE AND RC STRUCTURES

In this section some results of a symmetric notched beam (Fig. 3a), and of a reinforced concrete deep beam (DWT2) tested by Leonhardt and Walther [7] (Fig. 3b), are reported. The geometrical features of the notched beam are: total length 500 mm, span 450 mm, height 100 mm, thickness 50 mm and notch depth 10 mm; the distance between the loading points is 150 mm. Some different meshes were used for the analysis [2], referred to as very coarse, coarse, medium, fine and very fine, respectively. The material parameters were given by: Young's modulus $E_c = 38000 MPa$, Poisson's ratio $\nu = 0.2$, tensile strength $f_t = 3 MPa$, fracture energy $G_f = 60 N/m$.

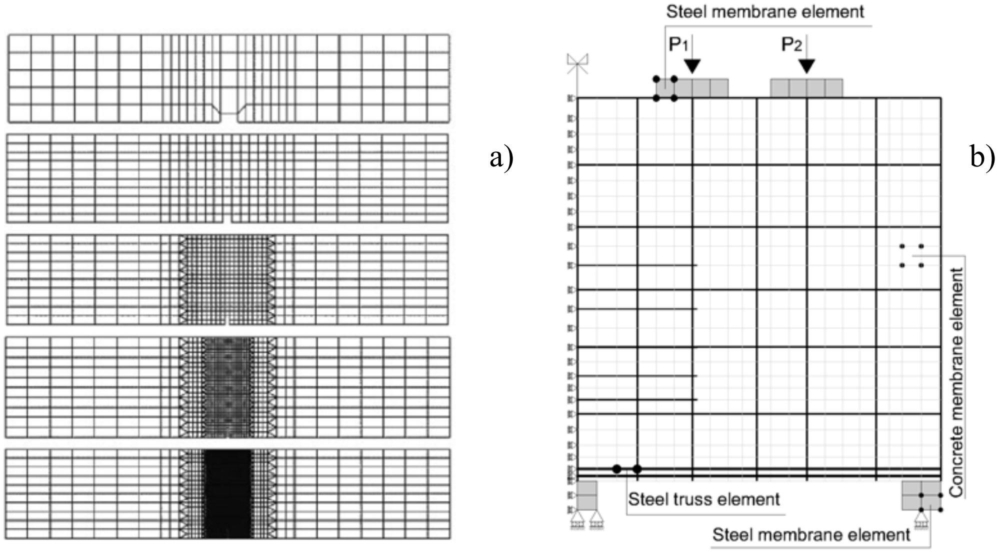

Figure 3. Meshes considered in the analyses of notched beam (a), and DWT2 beam (b).

In Fig. 4 the load versus deflection curves obtained by adopting non-linear tension softening are reported. The reference curves obtained from the NLFE analysis with the fixed smeared crack model based on the concept of total-strain is shown for good comparison. The procedure turns out to be simple. Moreover, as the element size decreases, or the total number of teeth *N* increases, the results improve, meaning that the approach is mesh-size objective.

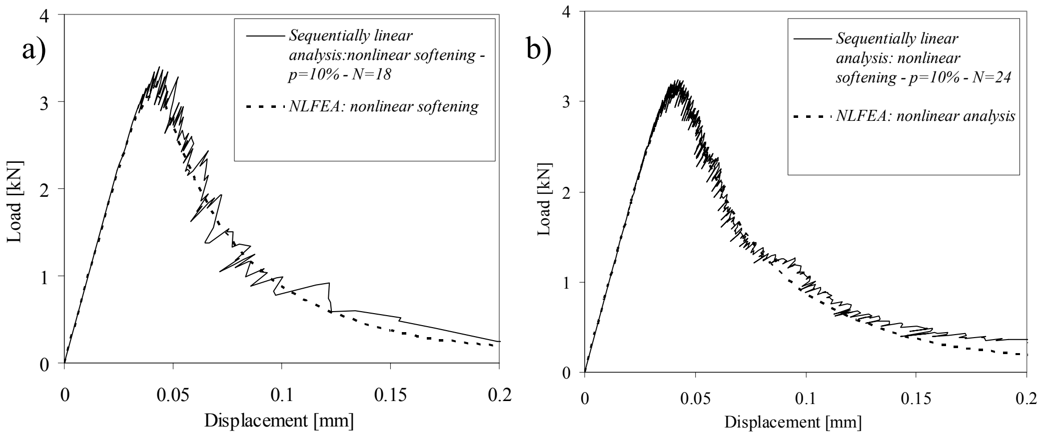

Figure 4. Notched beam: load-displacement diagram, nonlinear tension softening, coarse mesh (a), and fine mesh (b).

Exploiting symmetry, only one-half of the DWT2 beam has been analyzed, Fig. 3b. The beam is modeled by four-noded plane stress elements for the concrete and two-noded truss elements for the reinforcement. Perfect bond was assumed between the concrete and reinforcement. NLFE analyses have been carried out by adopting fixed smeared crack model, based on the concept of total-strain. The nonlinear analyses were performed under displacement control using regular Newton-Raphson. The load-deflection curve is shown in Fig. 5a. It is worth noting that the NLFE analysis exhibits a very sudden drop in step 30. Here, the NLFE analysis diverged and the convergence has not been reached after 100 iterations. At this increment step, a crack besides the supporting member suddenly appears, while yielding of longitudinal stirrups occurs at the same time, over the middle support. Beyond this critical point, the analysis could be partially continued and the cracks become wider at step 60. The obvious conclusion is that the standard incremental-iterative Newton-Raphson procedure is not capable of adequately catching the sudden, explosive cracking that occurred in the experiment.

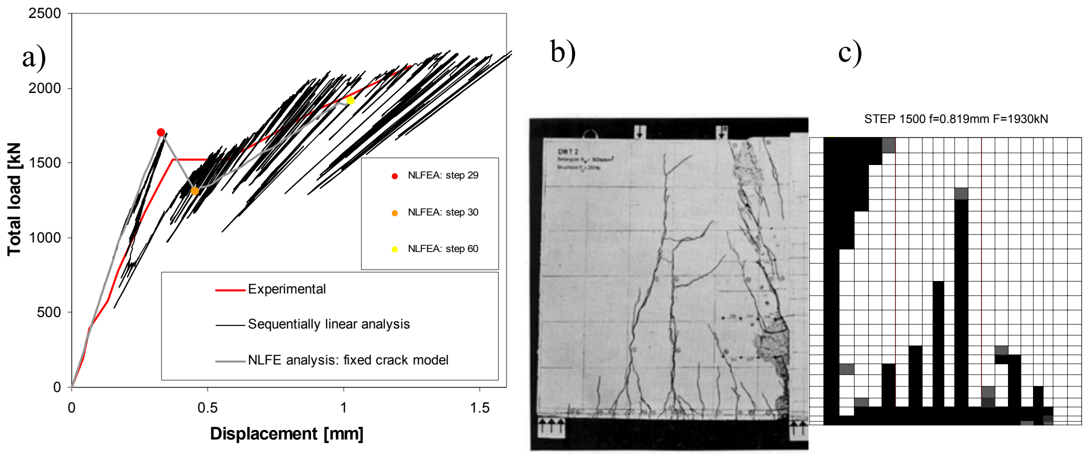

Figure 5. DWT2 load-deflection diagram (a), experimental crack pattern (b) and concrete damaged elements in tension (c) at final load F=1930 kN.

On the other hand, the same beam can be analyzed in the sequentially linear fashion. The sequentially linear analysis easily reveals what happens: a pronounced quasi-static snap-back behavior takes place revealing the very sudden and brittle development of the major vertical crack(s) close to the mid-support. This snap-back, together with the other ripples, appears automatically thanks to the scaling procedure. Fig. 5b shows the experimental crack pattern at failure, while the completely cracked concrete elements are shown in Fig. 5c.

More other reinforced concrete structures, studied with the sequentially linear approach, are presented in [8].

CONCLUSIONS

The results indicate that the sequentially linear method is capable of simulating brittle cracking and snap-backs, which are typical in plane concrete and RC structures. The approach always 'converges' as the secant saw-tooth stiffness is always positive definite. Divergence, often encountered with nonlinear FE analysis because of negative softening tangent stiffness, is avoided. The approach is stable and robust, therefore appealing to practicing engineers.

LIST OF NOMENCLATURE

$\varepsilon_{cr} = f_t / E$,
$f_{cm} = f_{ck} + 8$,
$G_F = G_{F0}(f_{cm}/10)^{0.7}$,
G_{F0} = base value of fracture energy which depends on the maximum aggregate size, as the value of α_F,
$w_c = \alpha_F (G_F / f_t)$,
$w_1 = 2G_F / f_t - 0.15 \cdot w_c$,
$A = (\delta w_c h - w_1 h)$
$B = [E(\delta w_c h - w_1 h)\varepsilon + E w_1 w_c - f_t w_1 h]$
$C = E f_t (w_1 w_c - w_1 h \varepsilon)$.

$$a = 4h^2 E_i \left[\left(\delta^2 w_c^2 + w_1^2 - 2\delta w_c w_1 \right) \left(E - E_i \right) \right]$$

$$b = 2h(\delta w_c - w_1)(2Ehf_{ct} w_1 + 2pEhf_{ct} w_1 + 2p\delta E_i hf_t w_c - 4pE_i hf_t w_1 - 2E_i hf_t w_1 + 2E_i E w_1 w_c)$$

$$c = f_t \left[4p\delta hE w_1 w_c^2 + 4p^2 \delta^2 h^2 f_t w_c^2 - 8p^2 \delta h^2 f_t w_1 w_c - 4p\delta h^2 f_t w_1 w_c - 4phE w_1^2 w_c + 4 \cdot p^2 \cdot h^2 \cdot f_t \cdot w_1^2 + \right.$$
$$\left. + 4ph^2 f_t w_1^2 - 4Ehw_1^2 w_c + h^2 f_t w_1^2 - h^2 w_1^2 + 4\delta Ehw_1 w_c^2 \right]$$

REFERENCES

1. Rots, J.G. (2001) In *Fracture Mechanics of Concrete Structures*, Proc. FRAMCOS-4, de Borst R, Mazars J, Pijaudier-Cabot G, van Mier JGM, Balkema AA (eds). Lisse: The Netherlands, 831-839.
2. Rots, J.G., Invernizzi, S. (2004) *Int. Journal for Numerical and Analytical Methods in Geomechanics*, **28**, 821-856.
3. Rots J.G., Belletti B., Invernizzi S. (2006). On the shape of saw-tooth softening curves for sequentially linear analysis. EURO-C 2006 Computational Modelling of Concrete Structures, 27-30 March, Mayrhofen, Tyrol, Austria, 431-442.
4. CEB-FIB Model Code 1990. Bulletin No. 213/214 (1993), Comite International du Beton.
5. Belletti B, Cerioni R, Iori I. (2001) *ASCE Journal of Structural Engineering*; **127(12)**, 1412-26.
6. Eurocode 2: Design of concrete structuree – Part 1: General rules and rules for buildings. CEN, 2002.
7. Leonhardt F., and Walter R. Wandartige Trager. Deutsher Ausschuss für Stahlbeton, D.A.f. St., Heft 178, Ernst & Sohn, Berlin, Germay, 1966.
8. Rots J.G., Belletti B., Invernizzi S. (2006). Simplified Saw-Tooth Softening Model for Reinforced Concrete Structures. Fib Congress 2006, 5-8 June, Naples.